for mutual distortion of their wave functions to occur. Thus, most DA spectra are quite unsuitable for an accurate determination of ϵ. The simplicity of the C+O spectrum is unique among those now available.

IV. TEMPERATURE DEPENDENCE OF DIELECTRIC CONSTANT

A comparison of our results with Barker's indicates a 3.3% increase, from 10.75 to 11.1, in the static dielectric constant of GaP between 1.6°K and room temperature, but direct measurements of the temperature dependence are insufficient to confirm this conclusion. The dielectric constant is the sum of electronic and lattice parts, ϵ_{el} and ϵ_{lat}, respectively, with $\epsilon_{el} > \epsilon_{lat}$. The contribution of the electronic part to the static dielectric constant $[\epsilon_{el}(0)]$ is obtained by measuring the refractive index ($\epsilon_{el}=n^2$) as a function of frequency, and then extrapolating to zero frequency. Pikhtin and Yas'kov made such measurements at 80 and 290°K.[12] They show an increase in $\epsilon_{el}(0)$ of only 1.5% between 80 and 290°K, but their results depend on a fairly long extrapolation. We know of no experimental work on the temperature dependence of ϵ_{lat}.

Faulkner has determined the low-temperature values of $\epsilon(0)$ for Si and Ge by fitting the absorption spectra of shallow donors.[13] His results indicate increases of 2.5 and 4.2%, respectively, for Si and Ge between liquid-helium and room temperature. These dielectric-constant increases are consistent with the refractive-index increases measured by Cardona, Paul, and Brooks.[13]

V. IONIZATION ENERGIES

Use of the new value $\epsilon=10.75$ in the analysis of DA spectra yields new values of E_D+E_A, in most cases about 2 meV higher than the values obtained with $\epsilon=11.1$. We now find $E_D+E_A=152$ meV for the shallow C+S pair spectrum. To split this energy between donor and acceptor we rely on Onton's value of 104 meV for the ionization energy of the donor S, obtained by analyzing the infrared excitation spectrum of S.[14] We therefore take $E_A(\mathrm{C})=48$ meV.[15] Combining this with the new value $E_D+E_A=943.5$ meV for the C+O spectrum, we obtain $E_D=895.5$ meV for the deep O donor. This value fits the photoexcitation spectrum of the O donor[16] significantly better than the lower estimate (893±2 meV) in Ref. 3.

[12] A. N. Pikhtin and D. A. Yas'kov, Fiz. Tverd. Tela **9**, 145 (1967) [English transl.: Soviet Phys.—Solid State **9**, 107 (1967)].

[13] R. A. Faulkner, Phys. Rev. **184**, 713 (1969); M. Cardona, W. Paul, and H. Brooks, J. Phys. Chem. Solids **8**, 204 (1959).

[14] A. Onton, Phys. Rev. **186**, 786 (1969).

[15] Acceptor ionization energies derived from the pair spectra are accurate to $\approx\pm1$ meV, mainly because of the uncertainty in E_g. Relative values are accurate to better than ±0.5 meV.

[16] P. J. Dean and C. H. Henry, Phys. Rev. **176**, 928 (1968).

PHYSICAL REVIEW VOLUME 188, NUMBER 3 15 DECEMBER 1969

Epitaxy of CdS on SrF_2

W. H. Strehlow and Earl L. Cook
Central Research Laboratories, 3M Company, St. Paul, Minnesota 55101

(Received 25 August 1969)

The epitaxy of wurtzite CdS on (111)-cleavage planes of SrF_2 is examined theoretically and experimentally. The theoretical treatment is based on the assumption that the predominent interaction across the film-substrate interface is of an ionic type. The energy of a unit of the CdS films interacting with the substrate is calculated by lattice summation as a function of position and orientation. Based on a minimum-energy criterion, the calculation shows that it is more favorable for a sulfur layer rather than a cadmium layer to be immediately adjacent to the substrate. Further, the calculation yields the positions on an atomic scale of the atoms of the deposit relative to those of the substrate. Epitaxial films of CdS on SrF_2 were grown using a chemical transport reaction and were shown to have the wurtzite structure with the [0001] direction of the deposit parallel to the [111] direction of the substrate. The $[1\bar{1}00]$ direction of the film is perpendicular to the $[10\bar{1}]$ direction of the substrate. An experimental investigation of the film surfaces using an ion-scattering method verified the prediction that a sulfur layer is immediately adjacent to the substrate.

I. INTRODUCTION

THE growth of epitaxial films of CdS on (111)-cleavage planes of CaF_2 and of CdSe on (111)-cleavage planes of CaF_2 and BaF_2 has been reported in the literature.[1–4] These reports deal primarily with the crystallinity of the films and the measurement of optical and electrical properties. There is little information available on the atomic arrangement at the film-sub-

[1] G. O. Müller and H. Peibst, Phys. Status Solidi **8**, K51 (1965).

[2] L. V. Al'tman, E. N. Vorontsova, Yu V. Ruban, and G. P. Tikhomirov, Kristallografiya **12**, 694 (1967) [English transl.: Soviet Phys.—Cryst. **12**, 601 (1968)].

[3] W. Kleber, I. Mietz, and U. Elsasser, Kristall Technik **2**, 327 (1967).

[4] R. Ludeke and W. Paul, Phys. Status Solidi **23**, 413 (1967).

strate interface. The investigation reported here is concerned with an atomistic model for the epitaxy of CdS on SrF_2, which assumes that the predominant interaction across the film-substrate interface is of an ionic type. Such a model predicts the positions of the cadmium and sulfur relative to the ions of the substrate. The subsequent examination of the CdS films on SrF_2 using ion-blocking [5–9] and ion-scattering[10–13] techniques allowed the experimental verification of certain of these predictions.

Cleaved crystals of SrF_2 are well suited for the epitaxial growth of wurtzite CdS. This material has the fluorite structure (Fig. 1) and exhibits a layered arrangement $\cdots$F-Sr-F-F-Sr-F$\cdots$ with a [111] crystallographic axis perpendicular to the layers.[14] Cleavage always occurs between two adjacent fluorine layers,[15] so cleaved surfaces are (111) planes with the outermost layer being a fluorine layer. Moreover, the cleaved surfaces are extremely flat with only occasional cleavage steps. The point symmetry around the [111] direction of the substrate is compatable with the point symmetry around the [0001] direction of the deposit.[14] Furthermore, assuming no relaxation of the surface, the spacing between surface fluorine ions according to the x-ray data is $\sqrt{2}a_0/2=4.101$ Å at 26°C; this compares favorably with the 4.137 Å spacing along the a axis of CdS.[14] Thus, it is reasonable that the epitaxial growth of CdS on SrF_2 occurs with the (0001) plane of the deposit parallel to the (111) plane of the substrate and the $[1\bar{1}00]$ direction in the deposit perpendicular to the $[10\bar{1}]$ direction in the substrate. The misfit for this case is 0.9% at 26°C and decreases to 0.2% at the deposition temperature.

The assumption of ionic-type interactions and the ideal geometry of CdS on SrF_2 allow an explicit calculation of the position of the deposit with respect to the substrate. For the most part, the calculation uses the methods of the classical ionic theory.[16–18] The classical picture of ionic solids is one of spherical ions containing integral numbers of electronic charges. The primary interaction is electrostatic and accounts for the binding of the crystal. Typically, the electrostatic energy agrees quite well with the observed cohesive energy; the difference is attributed mainly to van der Waals's and repulsive interactions. The predominant van der Waals interaction[19,20] is the dipole-dipole interaction and depends inversely on the sixth power of the ion separation. The repulsive or hard-core interaction results from the interpenetration of adjacent ions and depends exponentially on the ion separation according to Born and Mayer.[21]

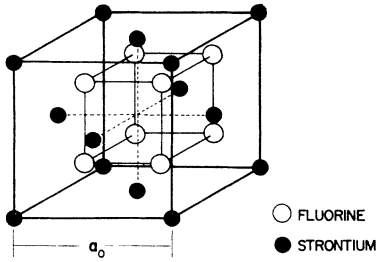

FIG. 1. Unit cell of the fluorite structure.

The details of the calculation are described in Sec. II. The experimental aspects are presented in Sec. III. The final section contains a brief discussion of the results.

II. THEORETICAL ASPECTS

Formulation of Equations

The essential difference between the present calculation for the epitaxy of CdS on SrF_2 and the usual cohesive energy calculations[16–18] is in the lattice summations and in the methods required to obtain convergence. This distinction is a mathematical one and does not involve any of the essential concepts of the model. Consequently, the details of the lattice summation can be presented before elaborating on the proposed model.

The difference in the two cases is readily understood by considering the calculation for an ideal solid. The electrostatic potential is given by

$$V(\mathbf{r})=\sum Z_i e\,|\mathbf{r}-\mathbf{r}_i|^{-1}, \qquad (2.1)$$

where $\mathbf{r}$ is a vector to the field point, $\mathbf{r}_i$ is a lattice vector, and $Z_i e$ is the charge on the ion located at $\mathbf{r}_i$. The series in Eq. (2.1) exhibits convergence problems and the evaluation by direct summation is impractical. Madelung[22] and others,[17,23–25] particularly Ewald,[23] have

[5] A. F. Tulinov, B. G. Akmetova, A. A. Puzanov, and A. A. Bednyakov, Zh. Eksperim. i Teor. Fiz. Pis'ma v Redaktsiya **2**, 48 (1965) [English transl.: Soviet Phys.—JETP Letters **2**, 30 (1965)].

[6] A. F. Tulinov, V. A. Kulikauskas, and M. M. Malov, Phys. Letters **18**, 304 (1965).

[7] A. F. Tulinov, Usp. Fiz. Nauk. **87**, 585 (1965) [English transl.: Soviet Phys.—Usp. **8**, 864 (1966)].

[8] R. S. Nelson, Phil. Mag. **15**, 845 (1967).

[9] R. Behrisch, Can. J. Phys. **46**, 527 (1968).

[10] W. H. Strehlow and D. P. Smith, Appl. Phys. Letters **13**, 34 (1968).

[11] D. P. Smith, Bull. Am. Phys. Soc. **11**, 770 (1966).

[12] D. P. Smith, J. Appl. Phys. **38**, 340 (1967).

[13] D. P. Smith, in The Thirteenth National Vacuum Symposium, San Francisco, 1966 (unpublished).

[14] R. W. G. Wyckoff, *Crystal Structures* (Wiley-Interscience, Inc., New York, 1963), 2nd ed., Vol. 1.

[15] L. Krastanow and I. N. Stranski, Z. Krist. **99**, 444 (1938).

[16] M. Born and K. Huang, *Dynamical Theory of Crystal Lattices* (Oxford University Press, New York, 1954), Chap. 1.

[17] M. P. Tosi, in *Solid State Physics*, edited by F. Seitz and D. Turnbull (Academic Press Inc., New York, 1964), Vol. 16, pp. 1–113.

[18] J. Sherman, Chem. Rev. **11**, 93 (1932).

[19] A. D. Crowell, in *The Solid-Gas Interface*, edited by E. A. Flood (Marcel Dekker, Inc., New York, 1967), Vol. 1, Chap. 7.

[20] J. O. Hirshfelder, C. F. Curtiss, and R. B. Bird, in *Molecular Theory of Gas and Liquids* (John Wiley & Sons, Inc., New York, 1954), Chap. 13.

[21] M. Born and J. E. Mayer, Z. Physik **75**, 1 (1933).

[22] E. Madelung, Z. Physik **19**, 524 (1918).

[23] P. P. Ewald, Ann. Physik **64**, 253 (1921).

[24] B. E. van der Hoft and G. C. Benson, Can. J. Phys. **31**, 1087 (1953).

[25] H. M. Evjen, Phys. Rev. **39**, 675 (1932).

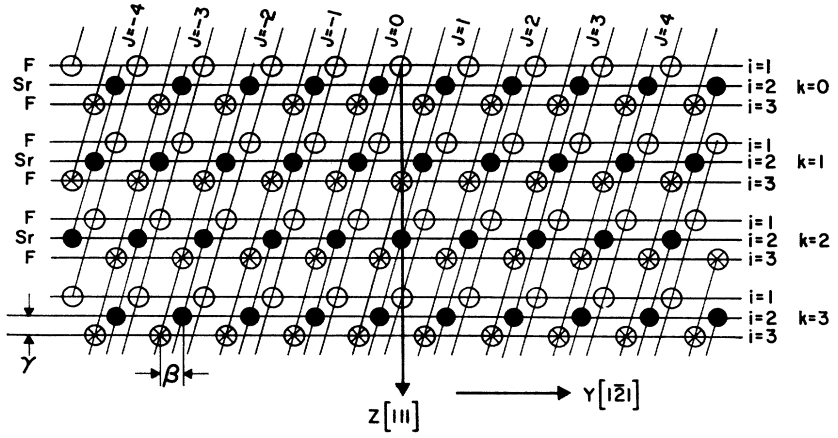

FIG. 2. Projection of the SrF_2 lattice onto the (10$\bar{1}$) plane showing the indexing for the lattice sums in Eq. (2.3).

devised methods which transform this series into a rapidly converging one. These transformations, for the most part, require the lattice to be strictly periodic in all three dimensions so that reciprocal-lattice expansions may be performed. They are not applicable to the case of a semi-infinite solid, i.e., a solid with a single-plane surface, since the surface destroys the three-dimensional periodicity and invalidates the reciprocal-lattice expansions. The method used to treat the surface case[22,24,26] supposes the lattice to be composed of lines of ions chosen so that periodicity exists in one dimension along these lines. Then a one-dimensional reciprocal-lattice expansion (a simple Fourier expansion) may be performed and a convergence-accelerating transformation applied.

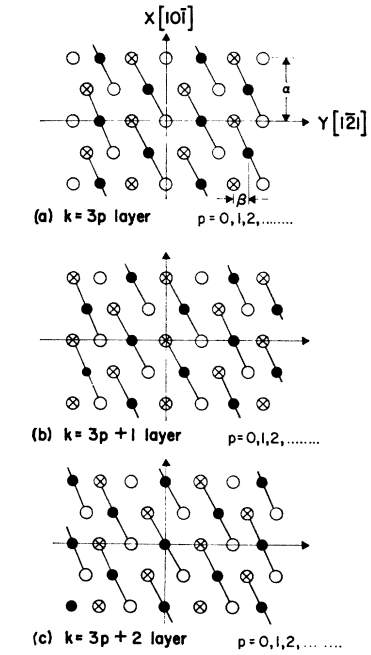

FIG. 3. Projections of the SrF_2 lattice onto the (111) plane for different values of k.

[26] F. G. Fumi and M. P. Tosi, Phys. Rev. 117, 1466 (1960).

The electrostatic potential due to a single line of point ions each with a charge $Z|e|$ is given by[22,24,26]

$$V(r)=2Z|e|\alpha^{-1}\{\sum_{l=1}^{\infty}2K_0(2\pi l\alpha^{-1}r^{(1)})\cos(2\pi l\alpha^{-1}r^{(11)}) +\ln(2\alpha/r^{(1)})+\lim_{N\to\infty}(\ln N)\}, \quad (2.2)$$

where $\mathbf{r}$ is a vector to the field point, N is an integer, α is the period along the line, $r^{(1)}$ is the component of $\mathbf{r}$ perpendicular to the line, $r^{(11)}$ is the component of $\mathbf{r}$ parallel to the line, and $K_0(x)$ is the modified Bessel function of the second kind.[27] Although the last term in Eq. (2.2) is undefined, it does not present any difficulties since it is independent of $\mathbf{r}$ and is thus identically zero whenever a combination of lines that is charge neutral is considered. Equation (2.2) is restricted to nonvanishing values of $r^{(1)}$; it is not applicable to points on the line. Further, the coordinate origin is assumed to coincide with a point on the line.

The application of Eq. (2.2) to the semi-infinite solid requires the resolution of the system into simply periodic lines of identical ions. The substrate thus resolved is illustrated in Figs. 2 and 3. The coordinate system used has the substrate-film interface in the xy plane and the z axis parallel to the [111] direction in the substrate. The x and y axis are parallel to the [10$\bar{1}$] and the [1$\bar{2}$1] directions, respectively. The lines of ions are parallel to the x axis with a periodicity along the line of $\alpha=\sqrt{2}a_0/2$, where a_0 is the lattice parameter of the substrate ($a_0=5.7996$ Å for SrF_2). Each pair of indices refers to a combination of two lines of fluorines and one line of strontiums, so the combination is charge neutral.

By making the appropriate changes in the coordinate origin and introducing the proper summations, Eq. (2.2)

[27] *Handbook of Mathematical Functions*, edited by M. Abramowitz and I. A. Stegun (U. S. Department of Commerce, National Bureau of Standards, Washington, D. C., 1964), Chaps. 9 and 10.

yields the total electrostatic potential above the surface of the substrate[28–30]:

$$V(\mathbf{r})=4|e|\alpha^{-1}\sum_{i=1}^{3}\sum_{j=-\infty}^{\infty}\sum_{k=0}^{\infty}\sum_{l=1}^{\infty}Z_iK_0(2\pi l\alpha^{-1}r_{ijk}^{(\mathrm{I})})\times\cos(2\pi l\alpha^{-1}r_{ijk}^{(\mathrm{II})})+2|e|\alpha^{-1}\sum Z_i\ln(2\alpha/r_{ijk}^{(\mathrm{I})}),\quad(2.3)$$

where

$$r_{ijk}^{(\mathrm{I})}=[(y_{ijk}-y)^2+(z_{ijk}-z)^2]^{1/2},$$
$$r_{ijk}^{(\mathrm{II})}=[x_{ijk}-x],$$
$$x_{ijk}=(i+j+k-1)\alpha/2,$$
$$y_{ijk}=(3j-k-i+1)\beta,$$
$$z_{ijk}=(4k+i-1)\gamma,$$
$$\alpha=\sqrt{2}a_0/2,$$
$$\beta=(\sqrt{6})a_0/12,$$
$$\gamma=\sqrt{3}a_0/12,$$
$$Z_i=-1,\ 2,\ -1.$$

Note that x_{ijk} appears only in trigonometric functions and is, therefore, invariant under additive constants that are integral multiples of α. This fact has been used in the above formulation.

The convergence of the series involving the Bessel functions is satisfactory and a reasonable number of terms produces acceptable accuracy. The logarithmic terms, however, do present problems for the convergence is very poor.

The convergence of the logarithmic terms may be improved by considering the identity[31]

$$\sum_{n=-\infty}^{\infty}\ln[1+d^2/(n+c)^2]=\ln\prod_{n=1}^{\infty}[1+d^2/(n+c)^2][1+d^2/(n-c)^2]+\ln[1+d^2/c^2]=\ln\left(\frac{\cosh(2\pi d)-\cos(2\pi c)}{2\sin^2(\pi c)}\right).\quad(2.4)$$

By reindexing the substrate as shown in Fig. 4, the sum of logarithmic terms becomes

$$S=\sum Z_i\ln(2\alpha/r^{(\mathrm{I})})=-\sum_{m=0}^{\infty}\sum_{n=-\infty}^{\infty}\sum_{i=1}^{3}\sum_{j=1}^{3}Z_i\ln[r_{ijmn}^{(\mathrm{I})}/2\alpha],\quad(2.5)$$

where

$$r_{ijmn}^{(\mathrm{I})}=\{[(3n+j-1)\beta-y]^2+[(12m+w_{ij})\gamma-z]^2\}^{1/2}$$

and

$$(w_{ij})=\begin{bmatrix}0&2&4\\9&5&1\\6&8&10\end{bmatrix}.$$

By interchanging the order of summation and introducing for convenience the quantities

$$c_j=\tfrac{1}{3}(j-1-y/\beta),$$
$$d_{ijm}=[(12m+w_{ij})\gamma-z]/3\beta,$$

the sum becomes

$$S=-\sum_{m=0}^{\infty}\sum_{j=1}^{3}\sum_{i=1}^{3}\tfrac{1}{2}Z_i\ln[\cosh(2\pi d_{ijm})-\cos(2\pi c_j)].\quad(2.6)$$

The terms involving 2α and $\sin^2(\pi c_j)$ are absent from this result since they are independent of the index i and, therefore, vanish when the sum over i is performed. Equation (2.6) converges quite rapidly and only a few terms are required to achieve the desired accuracy.

The predominant van der Waals interaction is the dipole-dipole interaction.[19,20] The expression for the energy of interaction between ions i and j separated a distance r_{ij} is

$$E_{ij}^{(\mathrm{vdW})}=-c_{ij}/r_{ij}^6,\quad(2.7)$$

with

$$c_{ij}=3\alpha_i\alpha_j\epsilon_i\epsilon_j/2(\epsilon_i+\epsilon_j),$$

where α_i and α_j are the static polarizibilities, and ϵ_i and ϵ_j are energies characteristic of the ions. It is in the determination of the constants ϵ_i and ϵ_j where most treatments differ. For the most part, the ϵ's are not too different from the appropriate ionization potentials. For example, London[32] takes ϵ_i equal to $h\nu_i$, where ν_i

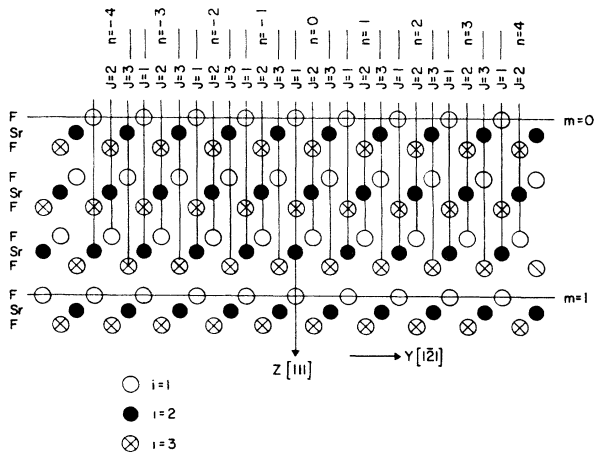

FIG. 4. Projection of the SrF_2 lattice onto the (10$\bar{1}$) plane showing the indexing for the lattice sums in Eq. (2.6).

[28] G. Bradistilov, Z. Krist. **102**, 26 (1939).
[29] G. Bradistilov and I. N. Stranski, Z. Krist. **103**, 1 (1940).
[30] G. C. Benson and E. Dempsey, Proc. Roy. Soc. (London) **A266**, 344 (1961).
[31] A. D. Wheelon, J. Appl. Phys. **25**, 113 (1954).
[32] F. London, Z. Physik **63**, 245 (1930).

TABLE I. van der Waals constants.

	α (Å^3)	ϵ (eV)
Cd^{++}	1.75	$0.75\times37.5=28.1$
Sr^{++}	1.76	$0.75\times43.0=32.3$
F^-	0.64	13.3
S^{--}	4.7	8.6
		c_{ij} (eV Å^6)
	Cd-F	15.2
	Sr-S	84.3
	Cd-Sr	69.3
	F-S	23.6

is the "main frequency" of the ion, while Born and Mayer[21] take the second ionization potential of the element for singly-charged positive ions and the electron affinity for negative ions. Mayer,[33] on the other hand, takes $\frac{3}{4}$ of the ionization potential for the positive ion, while Pitzer[34] suggests values which are nearly equal to twice the ionization potentials. The values of the parameters ϵ_i are presently quite uncertain.

The parameters used in the present work are in fair agreement with others.[30,33] The polarizibilities are those of Tessman, Kahn, and Shockley.[35] Following Mayer,[33] the characteristic energies ϵ in Eq. (2.7) are taken to be 0.75 of the third ionization potential[36] for the positive ions. For fluorine, the characteristic energy is obtained using Mayers formulation [Eq. (9) of Ref. 33 with $Q_{00}^2=1.44\times10^{-16}$ cm^2 and $\alpha=1.04\times10^{-14}$ cm^3]. For sulfur, the expression of Herzfeld and Wolf[37] is used

$$\epsilon=(h^2p/me^2\alpha)^{1/2}. \tag{2.8}$$

Here, p is the effective number of outer electrons and α is the polarizability. Mayer's value of 3.2 is taken for p. These values along with the constants c_{ij} of Eq. (2.7) are given in Table I.

The total van der Waals interaction may be obtained by summing Eq. (2.7) over the substrate. Although the sums are better behaved than in the electrostatic case, it is still beneficial to perform the transformation previously used to improve the convergence. Using the quantities defined in Eq. (2.3), the total van der Waals energy of the pth ion in the film at position $\mathbf{r}$ is[17]

$$E_p^{(\mathrm{vdW})}=\sum_{i=1}^{3}\sum_{j=-\infty}^{\infty}\sum_{k=0}^{\infty}c_{pi}\left\{\frac{3\pi}{8\alpha}[r_{ijk}^{(1)}]^{-5}\right.$$
$$+\pi^{1/2}[r_{ijk}^{(1)}]^{-5/2}\sum_{l=1}^{\infty}(2\pi l\alpha^{-1})^{5/2}$$
$$\left.\times K_{5/2}(2\pi l\alpha^{-1}r_{ijk}^{(1)})\cos(2\pi l\alpha^{-1}r_{ijk}^{(11)})\right. \tag{2.9}$$

The constant c_{pi} is given by Eq. (2.7).

[33] J. E. Mayer, J. Chem. Phys. **1**, 270 (1933).
[34] K. S. Pitzer, Advan. Chem. Phys. **2**, 59 (1959).
[35] J. R. Tessman, A. H. Kahn, and W. Shockley, Phys. Rev. **92**, 890 (1953).
[36] *Gmelins Handbuch der Anorganischen Chemie* (Verlag Chemie, Berlin, 1959), No. 33, p. 182; No. 29, p. 129, 1960.
[37] K. F. Herzfeld and K. L. Wolf, Ann. Physik **76**, 71 (1925).

Model for Epitaxy of CdS on SrF_2

The equations developed above are now applied to the epitaxial growth of CdS on SrF_2. The procedure is to consider a "unit of CdS" on the substrate surface and to calculate the combined electrostatic and van der Waals interaction energy as a function of the position and orientation of the unit on the substrate. (For reasons presented later, repulsive or hard-core interactions are not included in this calculation.) The location of the minimum energy is then interpreted as the preferred arrangement of the unit on the substrate. In view of this, the present approach is not concerned with the mechanisms by which the unit is formed, achieves the preferred arrangement, and coalesces into nuclei.

There are two types of CdS units; one for the case of the cadmium layer adjacent to the substrate, and one for the sulfur layer adjacent to the substrate. For both cases, the units are assumed to be consistent of four basal particles, forming a rhomb and participating in the interfacial layer, and one upper particle. This geometry is very suitable since the two layers of the film adjacent to the substrate can be composed of such units. In the film, each basal particle is shared by a total of four adjoining units, while the upper particle is not shared at all. The distance between the upper particle and the plane of the basal particles is given by $(1/2-u)c_0=0.841$ Å, where $u=0.375$ and $c_0=6.749$ Å for CdS.[14] An electrical charge that is a fourth of the nominal valence in CdS ($q=\pm1/2e$) is assigned to each basal particle while the upper particle has a charge equal to its nominal valence ($q=\mp2e$). Thus, the units are over-all charge neutral.

There are four assumptions required for the model: (1) The interactions are ionic or heteropolar, (2) the particles act as hard spheres with effective radii as given by Pauling, (3) the deposit does not perturb the substrate in any essential way, and (4) the substrate is atomically flat.

Elaborating on the first assumption, there are two possible ways that the CdS can be deposited: (1) with a cadmium layer adjacent to the substrate or (2) with a sulfur layer adjacent to the substrate. In the first case, the predominant pairing of particles across the film-substrate interface is between cadmium and fluorine. (Recall that the outermost substrate layer is a fluorine layer.) This interaction is primarily ionic as is indicated by the good correlation between the experimental value of the cohesive energy of CdF_2 and the value obtained from classical ionic theory (Table II). In the second case, the sulfur layer may be viewed as a substitute for the fluorine layer that would occur during the normal stacking in SrF_2. The sulfur would then be positioned above the strontium, and the interaction between sulfur and strontium is essentially ionic, as evidenced by the fair correlation between the experimental and theoretical values of the cohesive energy for SrS (Table II).

TABLE II. Cohesive energy calculation for SrF_2, CdF_2, and SrS.

	SrF_2	CdF_2	SrS
Structure	Fluorite	Fluorite	NaCl
A	11.6365	11.6365	3.4951
a_0 (Å)	5.800	5.388	6.020
K (10^{-12} cm²/dyne)	1.609	1.124	2.364
R_1 (Å)	2.511	2.333	3.010
R_2 (Å)	2.900	2.694	4.257
R_3 (Å)	4.101	3.810	a
M_1	8	8	6
M_2	6	6	12
M_3	12	12	a
V_c (Å³)	48.78	39.10	54.54
$f+-$	1.125	1.125	1.000
$f--$	0.750	0.750	0.500
$f++$	1.500	1.500	1.500
R_+ (Å)	1.130 (1.310)	0.970 (1.310)	1.130 (1.310)
R_- (Å)	1.360 (1.050)	1.360 (1.050)	1.840 (1.690)
b (10^{-12} ergs)	0.526 (0.957)	0.432 (0.956)	1.345 (1.332)
ρ (Å)	0.336 (0.328)	0.303 (0.289)	0.567 (0.557)
$E^{(e)}$ (kcal/mole)	−666.6	−717.6	−771.7
$E_1^{(r)}$ (kcal/mole)	63.9 (78.1)	55.4 (78.2)	108.3 (113.0)
$E_2^{(r)}$ (kcal/mole)	19.9 (5.4)	30.5 (8.0)	26.1 (22.0)
$E_3^{(r)}$ (kcal/mole)	1.4 (1.7)	1.6 (1.0)	a
E_{theory} (kcal/mole)	−581.4 (−581.4)	−630.1 (−630.4)	−637.3 (−637.7)
E_{expt} (kcal/mole)[b]	−584.	−661.9	−687.4
% difference	0.5	4.8	7.3
% ionicity[c]	89	74	43

[a] Third neighbors not considered for NaCl structure. [b] Reference 18. [c] Pauling, Ref. 38.

Table II gives the details of the cohesive energy calculation for SrF_2, CdF_2, and SrS. The pertinent equations and definitions are given in the Appendix. Note the correlation between the ionicity as calculated using Pauling's electronegativity and the difference between the calculated and experimental cohesive energies. This indicates that covalency is becoming appreciable in CdF_2 and SrS and, consequently, the classical ionic model is a progressively poorer approximation. Nevertheless, the numerical results show that the ionic model is satisfactory.

The choice of the crystal radii constitutes the second assumption. This is of importance because the spacing between the CdS film and the SrF_2 substrate is determined by the sum of the ionic radii between the nearest two interfacial particles. In other words, for purposes of obtaining the film-substrate separation, the ions are assumed to behave as hard spheres. The separation is consequently a function of the lateral position on the substrate. Clearly, the hard-sphere approach is an approximation, for the interfacial particles do actually interpenetrate, and the true separation is determined by the requirement that the energy be a minimum with respect to variations in the film-substrate separation. In the present work, Pauling's[38] crystal radii of the ions have been used.

The third assumption pertains to the early stages of the film growth where there is a negligible coverage of CdS. It is fair to assume that the perturbation of the substrate by the deposition is no greater than that associated with the transition from the bulk solid to the surface layer. The latter perturbation is thought to cause slight distortions ($<5\%$) in the first few layers, but this effect is not well understood and theoretical estimates are difficult to obtain.[39] These distortions along with an almost negligible misfit of less than 0.2% according to the lattice spacings and linear thermal expansion coefficients of the bulk material (Table III) are readily accommodated by a slight modification of the CdS units. The edge length of the rhomb formed by the four basal particles is then given by $\sqrt{2}a_0/2$, where a_0 is the substrate-lattice parameter.

The combined electrostatic and van der Waals contributions to the interaction energy of the two types of CdS units and the substrate are shown in Figs. 5 and 6. These plots give, in perspective, the energy as a function of the lateral location on the substrate. The expected threefold symmetry of the substrate surface is clearly evident, and definite minima are seen to exist. The location of these minima are the preferred

TABLE III. Physical constants for the substrate and deposit.

Structure	Nearest-neighbor distance in interfacial plane (Å)	Thermal expansion coefficient (deg^{-1})	% misfit at room temp.	% misfit at deposition temp.
CdS hex.-C_{6v}^4	4.137	5.0×10^{-6} [a]	0.9	<0.2
SrF_2 cub.-O_h^5	4.101	15.7×10^{-6} [b]		

[a] R. R. Reeber and B. A. Kulp, Trans. AIME 233, 698 (1965).
[b] D. B. Sirdeshmukh and V. T. Deshpande, Indian J. Pure Appl. Phys. 2, 405 (1964).

[38] L. Pauling, in *The Nature of the Chemical Bond* (Cornell University Press, Ithaca, N. Y., 1940), 2nd ed., Chap. 10.

[39] W. J. Dunning, in *The Solid-Gas Interface*, edited by E. A. Flood (Marcel Dekker, Inc., New York, 1967), Vol. 1, Chap. 9.

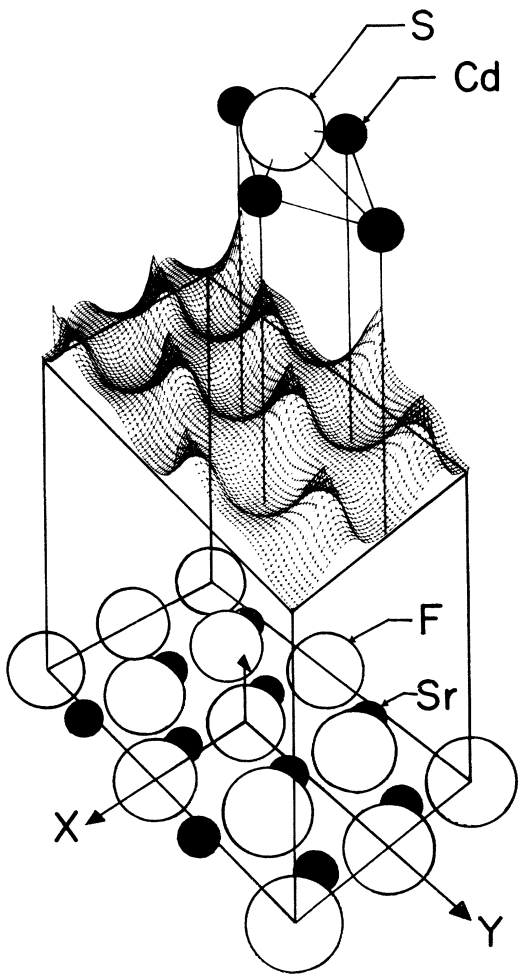

FIG. 5. Perspective view of the combined electrostatic and van der Waals energy as a function of the lateral position of the CdS unit for the case of a cadmium layer adjacent to the substrate.

locations of CdS on SrF_2 within the present assumptions. These plots show only one orientation for each of the CdS units. There are other possibilities obtained by rotating the units, but the cases shown in the figures are energetically more favorable.

Figure 7 gives the interaction energy as a function of y for a constant value of x passing through a minimum. From Figs. 5 and 7, it is seen that when the cadmium layer is adjacent to the substrate, the preferred arrangement is with cadmiums located over the fluorines and the upper sulfur located over a strontium. The film-substrate separation is determined by the "contact" between cadmium and fluorine, which, according to Pauling's crystal radii, is 2.33 Å. This is the smallest interionic spacing across the interface as well as the observed value of the cadmium-fluorine spacing in CdF_2 (Table II). The large peak seen in these figures results from the fact that the rather small cadmium (0.97 Å) will fit down into the interstice formed by three adjacent surface fluorines. This interstice is centered directly above the strontium. The sulfur is then located above the fluorine, and the large repulsion of the S-F and Sr-Cd interactions gives rise to the large peak. The value of the interaction energy at the minimum is −1.24 eV.

The case of a sulfur layer adjacent to the substrate is shown in Figs. 6 and 8. The minimum energy occurs when the sulfurs are over strontiums and the upper cadmium is over a fluorine. The film-substrate separation is determined by the sulfur which rests in the interstice formed by three surface fluorines. The sulfur-strontium spacing of 3.00 Å is very nearly equal to the crystal radii sum (2.97 Å), so the sulfur is essentially in contact with three flourines and a strontium. Furthermore, the strontium-sulfur spacing across the interface of 3.00 Å agrees favorably with the spacing of 3.01 Å observed in bulk SrS.[14] The value of the interaction energy at the minimum is −1.44 eV.

Several features of these results are noteworthy. First, since the minimum energy for sulfur-fluorine case

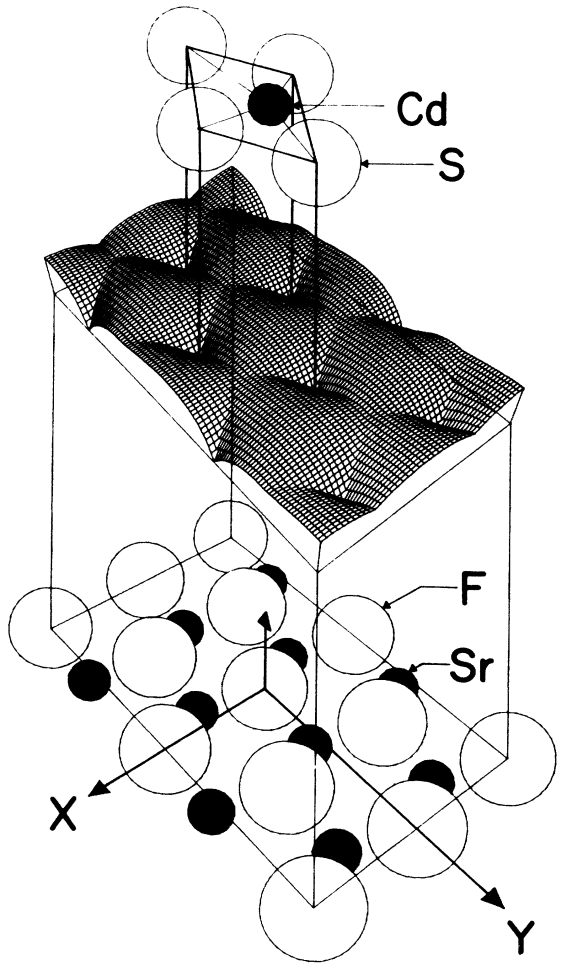

FIG. 6. Perspective view of the combined electrostatic and van der Waals energy as a function of the lateral position of the CdS unit for the case of a sulfur layer adjacent to the substrate.

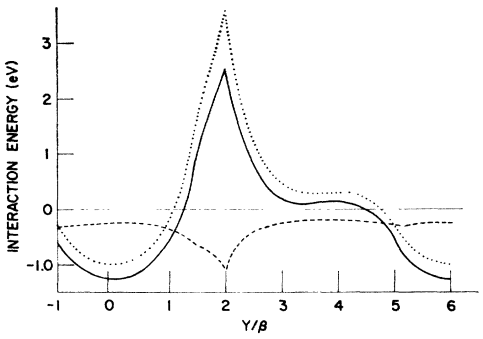

FIG. 7. Cross section parallel to the y axis through a minimum of Fig. 5 showing the total energy (solid), electrostatic energy (dotted), and van der Waals energy (dashed).

is smaller than the minimum energy for the cadmium-fluorine case, the growth of CdS on SrF_2 is predicted to occur with a sulfur layer adjacent to the interface. This ideally implies that the outermost layer of the deposit is a cadmium layer. Second, in both cases, the only regions which are attractive (i.e., interaction energy negative) are those around the minimum. In other words, there are no secondary minima, and there is no question as to the preferred location.

Thus far, the calculations show that the sulfur layer is adjacent to the uppermost layer of the substrate with the sulfurs located above the interstice formed by three surface fluorines. The second layer of the film consists of cadmium which are located above the fluorine of the uppermost layer of the substrate.

Repulsive Interaction

A negative value for the combined electrostatic and van der Waals interaction indicates that the CdS units are attracted to the substrate surface. This attraction is opposed by a force which results from the interpenetration of the interfacial ions. The inclusion of this interaction for CdS on SrF_2 is difficult. The problem is with the repulsive interaction between sulfur and fluorine, and to a lesser extent the interaction between strontium and cadmium. The first interaction is of the utmost importance, since sulfur-fluorine contacts occur quite frequently in the numerical evaluation of the model. In fact, the preferred location for the sulfur-fluorine interface case, according to the above, occurs with the sulfur in contact with three fluorines and one strontium.

The Born model[16,17,21] assumes that the repulsive interactions are two-body in character and have the form

$$E_{ij}^{(r)}=Be^{-r_{ij}/\rho}, \tag{2.10}$$

where B and ρ are parameters, and r_{ij} is the separation between the ith and jth ions. An alternative expression describes the interaction in terms of parameters associated with the individual ions rather than the pair:

$$E_{ij}^{(r)}=bf_{ij}b_ib_je^{-r_{ij}/\rho}, \tag{2.11}$$

with

$$b_i=e^{R_i/\rho}.$$

Here, R_i is the crystal radius of the ith ion and b is a parameter. The quantity f_{ij} in Eq. (2.11) is a factor suggested by Pauling[38] to better account for the configuration of the outer electrons in the two interacting ions:

$$f_{ij}=1+(z_i/n_i)+(z_j/n_j). \tag{2.12}$$

Here z_i is the valence of the ith ion, and n_i is the number of electrons in the outer shell. The parameters b and ρ are determined from the experimental compressibility and the equilibrium-lattice constant (cf. Appendix).

It is significant that the total repulsive energy is independent of the crystal radii used, but that the partitioning of this energy among the various ion pairs is extremely sensitive to the radii. This is illustrated in Table II; the values in parentheses are obtained using Huggins's radii,[29,40–42] while the others are obtained using Paulings radii.[38] For SrF_2, for example, the total repulsive interaction is 85.2 kcal/mole for both cases with first-neighbor interaction energies of 63.9 kcal/mole for Pauling's radii and 78.1 kcal/mole for Huggins's radii. The reason for this difference is readily understood by recalling that the crystal radii are introduced for convenience rather than for any fundamental theoretical reason. The usefulness of the concept lies in the fact that many ionic compounds behave as if the interionic spacings were the sum of the appropriate radii. The repulsive energy can then be uniquely partioned in a pairwise fashion so that any two ions interact in a completely predictable way. Stated another way, the Born model is not concerned with the atomistic details of the repulsive interaction and the partitioning of the energy, but rather it is concerned with a semiempirical expression for the total repulsive energy. As demonstrated so nicely by Benson and Dempsey,[30] the present state of the classical ionic theory does not allow an accurate statement about which of the several available crystal radii are correct.

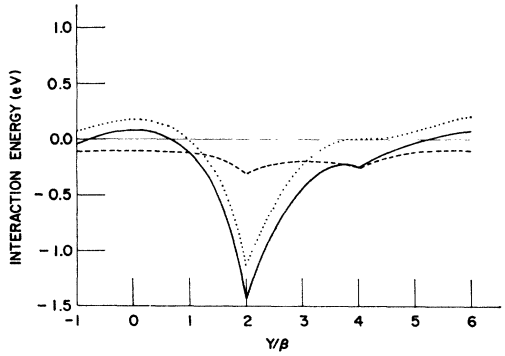

FIG. 8. Cross section parallel to the y axis through a minimum of Fig. 6 showing the total energy (solid), electrostatic energy (dotted), and van der Waals energy (dashed).

[40] M. L. Huggins and J. E. Mayer, J. Chem. Phys. **1**, 643 (1933).
[41] M. L. Huggins and Y. Sakamoto, J. Phys. Soc. Japan **12**, 241 (1957).
[42] M. L. Huggins, J. Am. Chem. Soc. **75**, 4126 (1953).

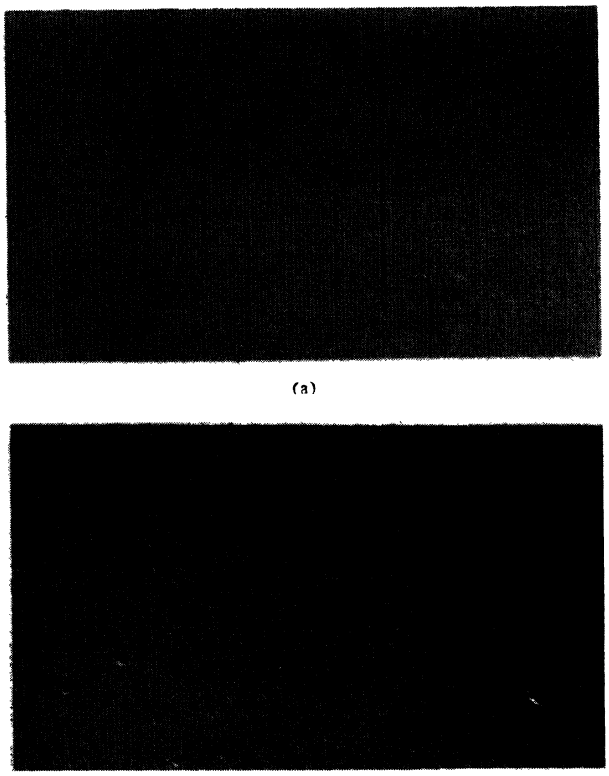

(a)

(b)

FIG. 9. Electron micrographs of (111) cleavage planes of SrF_2 showing cleavage steps: (a) The approximate step width is 1 μ and the step height 0.03 μ, and (b) the approximate step width is 0.1 μ and the step height 25 Å.

The evaluation of the Born model for CdF_2 and SrS provides an estimate for the Cd-F and Sr-S repulsive interactions (Table II). Unfortunately, the repulsive interactions between sulfur and fluorine and between strontium and cadmium cannot be determined so easily. First, there is the question of applicability of the Born model to the situation where ions of the same charge occur as nearest neighbors. Normally, nearest neighbors are of opposite sign and account for the majority of the interaction energy. Second and third neighbors are usually of the same sign, but these interactions account for only a small part of the repulsive interaction. Second, the only compounds with sulfur and fluorine as nearest neighbors are S_2F_2, SF_4, S_2F_{10}, and SF_6. All of these are gases at room temperature and exhibit the characteristics of covalent bonding. The Born model is not applicable. The only remaining approach is to extrapolate the results of other ionic compounds. In view of the other uncertainties of the Born model, principally the ionic radii, the results of an extrapolation would be too questionable to be of any value. It must be concluded, therefore, that the estimate of the S-F contribution to the repulsive interaction for CdS on SrF_2 cannot be obtained with the present theory and data. Nevertheless, the concept of using the repulsive parameters b and ρ, obtained from ionic compounds, to evaluate repulsive pair interactions across the interface is useful. For example, in the case of the epitaxial growth of alkali halides on fluorites the parameters b and ρ for the deposit[17] and substrate[30] are very similar and an extrapolation to all anion-anion and cation-cation pairs occuring across the interface is possible.

III. EXPERIMENTAL ASPECTS

The SrF_2 substrates were obtained commercially and cleaved into 1–2-mm-thick discs shortly before film growth. The cleaved surfaces showed well-ordered steps with an average step width of 1 μ and a step height of 0.03 μ, as shown in Fig. 9(a). A careful examination of these cleavage steps revealed that they are essentially atomically flat. By altering the cleaving procedure, the width and height of the steps could be varied. The substrate surface shown in Fig. 9(b) has steps that are only 25 Å high and 1000 Å apart. Again, the area along the steps is apparently atomically flat.

The CdS films were grown by the sandwich technique[43,44] using the transport reaction[45]

$$CdS(sol)+H_2(gas) \rightleftharpoons Cd(vap)+H_2S(gas). \quad (3.1)$$

The apparatus is arranged so that the source material (polycrystalline CdS) is maintained at a temperature greater than that of the substrate. Since the above reaction is endothermic when proceeding from left to right, the formation of cadmium vapor and H_2S prevails near the source, while the formation of CdS and H_2 is favored near the substrate. The geometry of the apparatus is such that the reactants remain in the region between the source and substrate, and the film growth is very efficient. The closeness of the source and substrate also allows some control over the final geometry of the film; it usually takes the shape of the source. The CdS films produced in this manner have a mirrorlike surface with occasional hexagonal structures similar to those observed by Weinstein and Wolff.[46]

Normally, the deposited film does not cover the substrate completely. Such a film does not show a sharp edge but rather a gradual transition from the continuous film to the bare substrate. In this region, varying degrees of film continuity exist, and this offers a unique opportunity for examining the growth process. Figure 10 shows three different sections of the transition region. The regular-shaped nuclei in Figs. 10(a) and 10(b) clearly show a high degree of alignment. The sharp edges of the nuclei form angles of 120° with each other and are parallel to the [10$\bar{1}$]

[43] E. Sirtl, J. Phys. Chem. Solids **24**, 1285 (1963).
[44] F. H. Nicoll, J. Electrochem. Soc. **110**, 1165 (1963).
[45] H. Schäfer, in *Chemical Transport Reactions* (Academic Press Inc., New York, 1964), p. 55.
[46] M. Weinstein and G. A. Wolff, J. Phys. Chem. Solids Suppl. **1**, 537 (1967).

directions of the substrate. This is a clear indication of the strong ordering effect of the substrate. This ordering is also apparent in the almost continuous film of Fig. 10(c).

The orientation of the CdS films was determined through electron diffraction and proton-blocking studies. The results in both cases show that the films are single crystalline and have the wurtzite structure with the [0001] direction of the deposit parallel to the [111] direction of the substrate and the $[1\bar{1}00]$ direction of the deposit perpendicular to the $[10\bar{1}]$ direction of the substrate.

The proton-blocking method[5–9] is based on back-scattered protons which emerge fairly uniformly from the surface of the sample except in those directions for which channeling occurs. The angular distribution of the back-scattered protons or the "blocking pattern" is uniquely related to the crystal structure at the surface. This method is ideally suited to the study of thin film because the incident protons penetrate only a short distance (<50 Å). In the present application, the calculated blocking pattern[47] was used to establish the structure of the epitaxial film. Further verification was provided by a blocking pattern obtained from a bulk single crystal of CdS that had been oriented through x-ray analysis.

One of the predictions of the numerical calculations presented above is that the CdS film should grow with the sulfur layer immediately adjacent to the substrate. This implies that the outer layer of the film should be a cadmium layer. Thus, an experimental determination of the crystallographic polarity of the CdS film grown on SrF_2 is of the utmost importance.

The method of determining the crystallographic polarity of a CdS single crystal by ion scattering has been recently reported.[10] This method is based on the energy distribution of the scattered ions, while the ion blocking utilizes the angular distribution. Ion scattering is, a result of the detection method, sensitive mainly to the first layer of atoms. The procedure is to scatter monoenergetic ions from the surface and to energy analyze the scattered ions. Typically, the energy distribution shows discrete peaks whose energy is simply related to the mass of the surface particles. This method is particularly suited to the determination of the polarity of thin films where the techniques such as etching are unsuccessful. In using this method, a beam of 2-keV He^+ ions was incident in the $(11\bar{2}0)$ plane of the CdS film at an angle of 45° from the normal. The ions scattered through an angle of 90° were energy analyzed. The beam-current density of 100 $\mu A/cm^2$ and a background pressure of 10^{-9} Torr was sufficient to assure that the sample remained free of absorbed contaminants.

Using ion scattering, the outermost layer of the CdS films was found to be composed of cadmium. Ideally, this result implies that the layer adjacent to the interface must be sulfur.

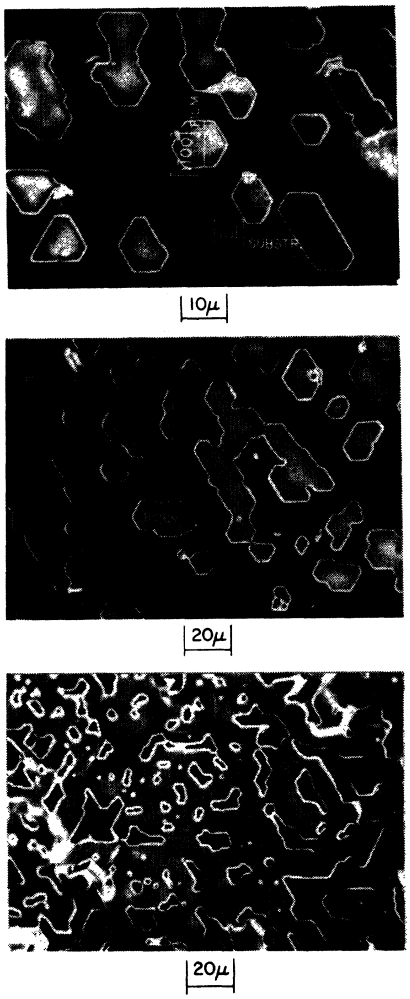

FIG. 10. Phase-contrast micrographs showing varying degrees of continuity of CdS films on SrF_2, and indicating the strong ordering effect of the substrate. (CdS deposit appears light while the SrF_2 substrate appears dark.)

In order to further support this result, the interfacial layer was examined directly. The film was removed from the substrate by first attaching a glass slide to the outer face of the film with an epoxy adhesive. After soaking the combination in distilled water at room temperature for several days, the substrate was easily removed from the film-glass-slide arrangement. From solubility data for CdS in water (10^{-10} moles/liter at 26°C), it was estimated that less than a monolayer of the CdS was dissolved during this procedure. An electron-microscopic examination of the inner surface revealed that very little damage of the film occurred during the stripping process. The impressions of the cleavage steps were clearly visible. Further, the crystallinity and orientation of the inner surface as determined

[47] E. L. Cook (unpublished).

by ion blocking indicated that the film was still single crystalline and had the expected orientation.

The inner surface of the stripped CdS film was found to be composed of sulfur by the ion-scattering method. This is a complete agreement with the polarity obtained from the outer surface.

IV. DISCUSSION

In spite of the vast amount of data reported on epitaxy, only a few experimental determinations of the binding energies of the film to the substrate have been published. From the measurement of the nucleation rate at various substrate temperatures, Walton *et al.*[48] have inferred, for instance, that the binding energy of a silver atom to the (100)-cleavage plane of sodium chloride is about 0.4 eV. Apparently, no theoretical calculations of the binding energy have been previously reported.

Within the scope of the classical theory of ionic solids, the combined electrostatic and van der Waals contributions to the binding energy of CdS on SrF_2 have been calculated. The present theory cannot provide a confident estimate of the repulsive contribution. However, it is reasonable to assume that the repulsive interaction is not greater than 50% of the total binding energy. Based on this assumption the total binding energy of CdS on SrF_2 is calculated to be about 1 eV. This value is considerably greater than the 0.4 eV that Walton *et al.* have obtained for a silver atom on sodium chloride. However, it must be remembered that this latter case does not involve the large electrostatic contribution associated with ionic bonding. Most likely, Walton's value should be compared with the van der Waals contribution to the total binding energy of CdS on SrF_2 of 0.31 eV.

The existing theories[49] of nucleation are all thermodynamic in nature and are concerned with the effect of the size of clusters on the nucleation rate. These theories suffer from a common deficiency: The assumption that thermodynamic properties may be ascribed to small clusters of adsorbed particles. Within these theories, the important factors are the relevant surface energies, namely, the substrate surface energy, the deposit surface energy, and the energy of the interface between the substrate and deposit. The last of these is the dominating factor, and the lack of data for this energy is responsible for the serious limitation in the understanding of nucleation phenomena.[49] The present approach provides values for the energy of the interface between the substrate and the deposit.

[48] D. Walton, T. N. Rhodin, and R. W. Rollins, J. Chem. Phys. **38**, 2698 (1963).

[49] D. W. Pashley, Advan. Phys. **14**, 327 (1965).

ACKNOWLEDGMENT

The authors would like to thank David P. Smith of our laboratories for performing the ion-blocking and ion-scattering experiments and for consulting with us regarding the results.

APPENDIX

The cohesive energy for an ideal solid is given by

$$\varphi = E^{(e)} + E^{(\mathrm{vdW})} + E^{(r)} + E^{(0)}. \tag{A1}$$

Here, $E^{(e)}$ is the electrostatic energy and is given by

$$E^{(e)} = -ZeA/a_0, \tag{A2}$$

where Ze is the smallest ionic charge in the lattice, A is the Madelung constant, and a_0 is the lattice constant. The repulsive interaction energy for the NaCl structure through second neighbors is

$$\begin{aligned} E^{(r)} &= E_1{}^{(r)} + E_2{}^{(r)} \\ &= M_1 b f_{+-} b_+ b_- e^{-r_1/\rho} \\ &\quad + \tfrac{1}{2} M_2 b (f_{++} b_+{}^2 + f_{--} b_-{}^2) e^{-r_2/\rho}, \end{aligned} \tag{A3}$$

and for the fluorite structure through third neighbors

$$\begin{aligned} E^{(r)} &= E_1{}^{(r)} + E_2{}^{(r)} + E_3{}^{(r)} \\ &= M_1 b f_{+-} b_+ b_- e^{-r_1/\rho} + \tfrac{1}{2} M_2 b f_{--} b_-{}^2 e^{-r_2/\rho} \\ &\quad + \tfrac{1}{2} M^3 b (f_{--} b_-{}^2 + f_{++} b_+{}^2) e^{-r_3/\rho}. \end{aligned} \tag{A4}$$

Here, M_i is the number of ith neighbors and r_i is the separation between ith neighbors.

The parameters b and ρ are determined from experimental values of the compressibility and equilibrium lattice constant. The equations for this calculation are

$$\begin{aligned} &d\varphi/da_0 = 0 \\ &\text{and} \\ &1/K = (a_0{}^2/9V)(d^2\varphi/da_0{}^2), \end{aligned} \tag{A5}$$

where K is the observed compressibility and V is the volume of the unit cell. This method for determining the repulsive parameters is simpler than some.[17] The more complex treatments consider temperature and pressure derivatives of the compressibility. These refinements are not warranted in view of the uncertainties which exist in the values of the many parameters. Furthermore, the Born model is, contrary to popular interpretation, semiempirical and it is not expected to account for second-order effects.[16,17]

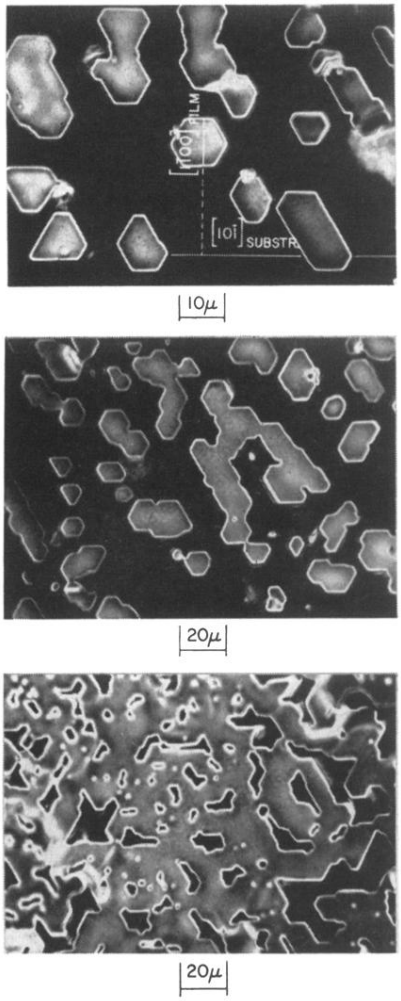

FIG. 10. Phase-contrast micrographs showing varying degrees of continuity of CdS films on SrF_2, and indicating the strong ordering effect of the substrate. (CdS deposit appears light while the SrF_2 substrate appears dark.)

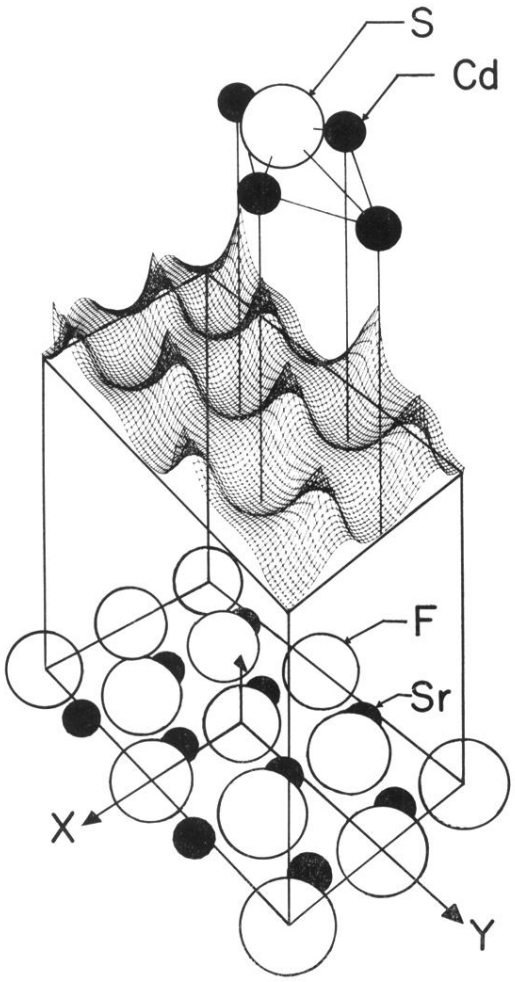

FIG. 5. Perspective view of the combined electrostatic and van der Waals energy as a function of the lateral position of the CdS unit for the case of a cadmium layer adjacent to the substrate.

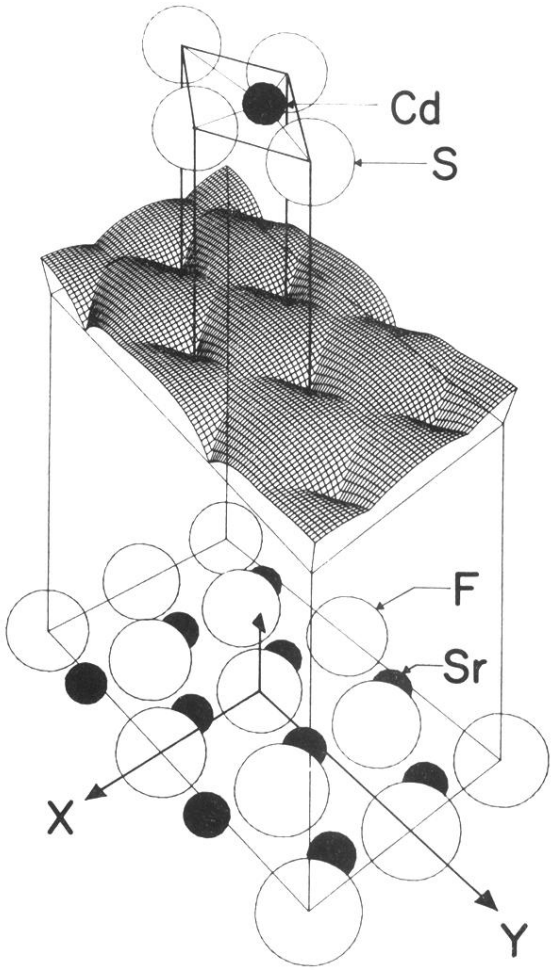

FIG. 6. Perspective view of the combined electrostatic and van der Waals energy as a function of the lateral position of the CdS unit for the case of a sulfur layer adjacent to the substrate.

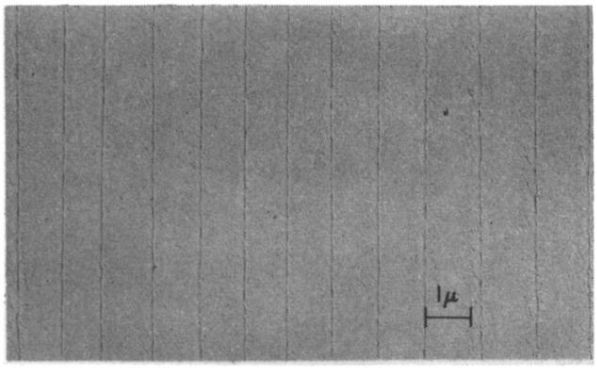

(a)

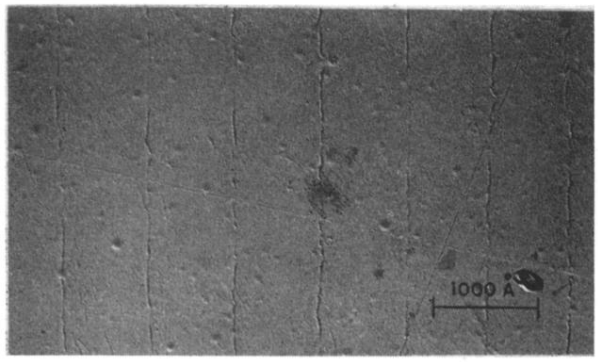

(b)

FIG. 9. Electron micrographs of (111) cleavage planes of SrF_2 showing cleavage steps: (a) The approximate step width is 1 μ and the step height 0.03 μ, and (b) the approximate step width is 0.1 μ and the step height 25 Å.